Proceedings of the 12th International IEEE Conference on Intelligent Transportation Systems, St. Louis, MO, USA, October 3-7, 2009

Exploiting LIDAR-based Features on Pedestrian Detection in Urban Scenarios

Cristiano Premebida, Oswaldo Ludwig and Urbano Nunes

Abstract— **Reliable detection and classification of vulnerable road users constitute a critical issue on safety/protection systems for intelligent vehicles driving in urban zones. In this subject, most of the perception systems have LIDAR and/or Radar as primary detection modules and vision-based systems for object classification. This work, on the other hand, presents a valuable analysis of pedestrian detection in urban scenario using exclusively LIDAR-based features. The aim is to explore how much information can be extracted from LIDAR sensors for pedestrian detection. Moreover, this study will be useful to compose multi-sensor based pedestrian detection systems using not only LIDAR but also vision sensors. Experimental results using our data set and a detailed classification performance analysis are presented, with comparisons among various classification techniques.**

I. INTRODUCTION

This article deals, in general terms, with the apparently simple issue: is it possible to perform pedestrian detection/classification using only LIDAR-based features? Before to answer this question, a detailed analysis of a set of classification techniques based on LIDAR features will be presented. Although many perception systems relies on vision-based modules for pedestrian classification in urban scenarios, our research is aimed towards developing a perception framework that uses information from LIDAR sensors to perform pedestrian classification. The range information is summarized by a set of LIDAR features, in some cases referred as geometrical features, calculated per segment/cluster, that characterizes the detected pedestrians.

Pedestrian detection is here considered as a part of a perception system, as shown in Fig. 1, composed by the following modules: data preprocessing, tracking and data association, feature extraction and pedestrian detection. More specifically, the objective of the present work is to emphasize the feature extraction and the feature selection modules, that are detailed in Section III, and pedestrian classification algorithms, described in Section IV. Tracking and data association have been treated on a previous work [1], and data preprocessing is succinctly described in Section II.

Any pedestrian protection system [2] to be implemented in a realistic situation should have the detection rate as higher as possible and, on the other hand, the number of false alarms would be under a reasonable value. The trade-off between detection and false positive rate is a particular challenge to be solved adequately. One solution that could be devised is the utilization of a LIDAR-based classifier acting as a complementary and redundant detection system, instead of a prior-detection or hypothesis generation system. This subject constitutes one of the main motivations of this work.

Previous works on pedestrian detection using LIDAR data can be divided in two communities[1] that differentiate in many aspects, some of them here described:

1) Mobile robotics: in most of the cases it is related to indoor scenarios, with pedestrians walking at low-speed; the perception range are usually short distances; the environment conditions are less prone to spurious interferences; usually non-pedestrians objects have a static behavior (except other robots); among others. Nevertheless, the complexity of the solutions are still challenging and the safety attributes are a critical issue.
2) Intelligent vehicles: the environment is outdoors, with pedestrians presenting many different behaviors; the perception range is a critical aspect to take into account and depends directly on the ego-vehicle velocity; the surrounding and the environmental conditions are numerous; the non-pedestrians entities vary tremendously in terms of characteristics and attributes, and the safety consideration is a mandatory aspect to be considered.

Despite the differences both cases can be analyzed considering a common functional diagram, as illustrated in Fig. 1, and most of the techniques used for a particular case can be adapted for the other one. This justifies the references on human detection systems developed within the mobile robotics community [3], [4].

In the intelligent vehicles community, some relevant works on object classification in urban scenarios using only 2D-LIDAR data are [5], [6], [1], [7]. The combination of range and image-based features/descriptors in sensor-fusion systems are described in [8], [9], [10].

In this paper we address pedestrian detection in urban areas using only features extracted from data gathered by a LIDAR, mounted in a vehicle moving at relatively low speed (up to 40Km/h). Additionally we propose new laser-based features that, in conjunction with some features presented in [3], are used to classify pedestrians on data sets containing data from an Ibeo Alasca XT and a Sick LMS200. The data sets are online available for public usage and for further comparisons. We also emphasize the importance on using a feature selection method that is independent of any specific classification method. Moreover, a set of classifiers are compared in terms of the Area under ROC curve (AUC) and

The authors are with the Department of Electrical and Computer Engineering, Institute of Systems and Robotics, University of Coimbra, Portugal. {cpremebida,oludwig,urbano}@isr.uc.pt

[1]Industry applications could be considered as a mobile robotics case.

978-1-4244-5521-8/09/$26.00 ©2009 IEEE

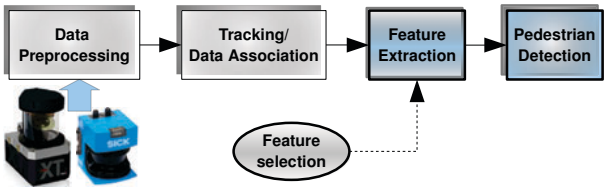

Fig. 1. Functional diagram illustrating the common modules in a LIDAR-based perception system for pedestrian detection. Along this paper, the bold blocks will be emphasized.

accuracy (Acc), and whose results are presented in Section V. These are the main contributions of the present work.

II. DATA PREPROCESSING

The raw range-points have to be processed in advance before the calculation of the feature vector and the subsequent object classification. The tasks performed in this preprocessing module are: pre-filtering, coordinate transformation, and segmentation.

Prefiltering aims to filter the incoming raw data in order to detect isolated/spurious range-points, to discard measurements that occur out a predefined field of interest, and to perform any pertinent task to reduce the complexity and the processing-time. Coordinate transformation, in our case, is a conversion from polar to the Cartesian coordinates, and finally the segmentation stage, which constitutes a critical part in such perception systems, can be performed by means of specific methods as presented in [6], [11], [8].

For allowing a better generalization of the methods presented here, all the range information were considered as two-dimensional measurements; that is the case of the Sick LMS/LD lasers. For multi-layers LIDAR (*e.g.* Ibeo Alasca), one can project the scanned points to a single reference plane.

Expressing a 2D full scan as a sequence of $N_{\mathcal{S}}$ measurement points in the form $Scan = \{(r_l, \alpha_l) | l = 1, ..., N_{\mathcal{S}}\}$, where (r_l, α_l) denotes the polar coordinates of the l^{th} *scan point*, a group of scan points that constitute a segment S_k can be expressed as

$$S_k = \{(r_n, \alpha_n)\}, \quad n \in [l_i, l_f], \quad n = 1, \ldots, np \qquad (1)$$

where np is the number of points in the current segment, l_i and l_f are the initial and the final scan points that define the segment. A segment can also be defined in Cartesian coordinates $\mathbf{x} = (x_k, y_k)$, where $(x_k = r_n \cos \alpha_n, \quad y_k = r_n \sin \alpha_n)$. Henceforth, a *segment* is explicitly related to a group of range-points related to one, unambiguously, object of interest and expressed by S_k.

As the objective of this paper is to demonstrate the feasibility on pedestrian detection based on features calculated from laser segments, all the experiments were conducted using data sets where the segments were extracted under user supervision, avoiding some problems invariably presented on realistic situations, such as: data association errors, over-segmentation, measurements missing, tracking inconsistencies, etc. Therefore, our interest is in the situation where an entity, pedestrian or non-pedestrian, has been already detected and the referred detected object, characterized as a segment, should be classified.

TABLE I
LIDAR FEATURES FOR PEDESTRIAN DETECTION.

f_i	Formula	Description
1	$np \cdot r_{min}$	r_{min} is the minimum range distance
2	np	Number of points
3	$\sqrt{\Delta X^2 + \Delta Y^2}$	Normalized Cartesian dimension
4	$\sqrt{\frac{1}{np}\sum_{n=1}^{np} \|\mathbf{x}_n - \bar{\mathbf{x}}\|}$	Standard deviation: $\mathbf{x}_n$ is the range-points array and $\bar{\mathbf{x}}$ the centroid
5	Radius $\leftarrow$ fitted circle	Radius: denotes the radius of a circle extracted from $\mathbf{x}_n$ using Guivant's method [12]
6	$\frac{1}{np}\sum_{n=1}^{np} \|\mathbf{x}_n - \tilde{\mathbf{x}}\|$	Mean average deviation from the median $\tilde{\mathbf{x}}$
7	IAV	The Inscribed Angle Variance (IAV), proposed by [4]
8	$std(f7)$	Standard deviation of the inscribed angles
9	$\frac{1}{np}\sum_{n=1}^{np} (\mathbf{x}_n - \hat{\mathbf{x}}_{l,n})^2$	Linearity (see [3]), where $\hat{\mathbf{x}}_{l,n}$ corresponds to the fitted line
10	$\frac{1}{np}\sum_{n=1}^{np} (\mathbf{x}_n - \hat{\mathbf{x}}_{c,n})^2$	Circularity (see [3]), with $\hat{\mathbf{x}}_{c,n}$ corresponding to the fitted circle
11	$\sum_{n=1}^{np} \frac{(\mathbf{x}_n - \mu_{\mathbf{x}})^2}{np}$	2^{th} central moment; $\mu_{\mathbf{x}}$ is the mean
12	$\sum_{n=1}^{np} \frac{(\mathbf{x}_n - \mu_{\mathbf{x}})^3}{np}$	3^{th} central moment
13	$\sum_{n=1}^{np} \frac{(\mathbf{x}_n - \mu_{\mathbf{x}})^4}{np}$	4^{th} central moment
14	$\sum_{n=1}^{np} \|\mathbf{x}_n - \mathbf{x}_{n-1}\|$	Segment length (see [3])
15	$std(f14)$	Standard deviation of the segment length

III. FEATURE EXTRACTION

Feature extraction from LIDAR data and its utilization for pedestrian detection in urban environment is a subject that has not been investigated significantly, although some works are worth of mention: [6], [1], [10]. Nevertheless, in the mobile robotics field, the work by [3] is a reference on using purely LIDAR features[2] for human detection in indoor environments. The components of the feature vector, many of them based on Arras's work, are summarized in Table I.

The feature vector extracted from a segment S_k is calculated using only 2D information in polar and/or Cartesian space, hence as said previously for the case of a multi-layer LIDAR the "vertical" information has to be projected on a common 2D plane, which means that all these features can be used in case of single-layer lasers. As a demonstration of a pedestrian detected by the LIDAR, with its corresponding segment and the region of interest (ROI) in the image plane, consider Figure 2. The related laser-features are highlighted in the left part of the Figure.

An important aspect when designing a classifier is to decide the features to be used and, if possible, the combination

[2]The object speed could be considered an exception.

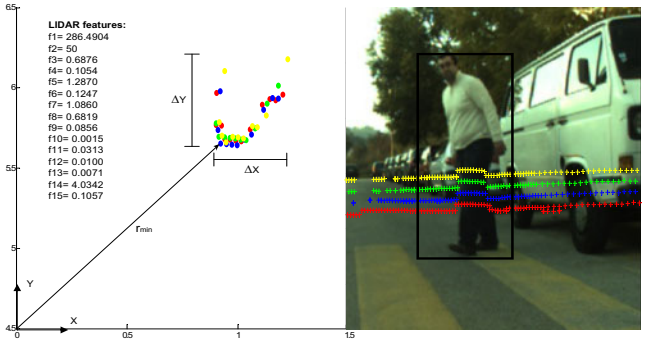

Fig. 2. An example that illustrates a pedestrian perceived by the laser, as a segment of range points, and the corresponding laser-features. The image is depicted to facilitate the understanding of the scene.

in which it will be applied during the classification process. To prevent redundancy and to take advantage of the diversity among the features, an approach based on mutual information was used for feature selection. We have adopted the method named mRMR (minimum-redundancy maximum-relevancy) [13] which is based on information theory. Instead of maximizing the dependency $maxD(S,c)$ directly, where S is the feature set which jointly have the largest dependency on the target class c, Peng developed his method based on maximal relevance criteria, which approximates $maxD(S,c)$ using the mean value of the mutual information $I(f_i/c)$ taken from individual features f_i:

$$maxD(S,c), D = \frac{1}{|S|}\sum_{f_i \in S} I(f_i/c) \tag{2}$$

Moreover, together with the max-relevancy, the mRMR method combines another condition to obtain mutually exclusive features. The later criteria is based on the minimal redundancy $minR(S)$ among the features:

$$minR(S), R = \frac{1}{|S|^2}\sum_{f_i, f_j \in S} I(f_i, f_j) \tag{3}$$

Those features with maximum relevancy and minimal redundancy using the Ibeo laser data set are (refer to Table I): f_i=[1,10,15,6,4,3,9,12,11,5,13,7,14,8,2], and those using the Sick laser: f_i=[1,10,15,8,14,11,9,5,12,13,2,6,4,7,3]. These sequence of features were used during the classifier's validation to determine the number of features with the best performance in terms of the area under ROC curve (AUC) and accuracy (Acc); the results are present in Subsection V-B. It is important to note that these sequences of features are independent, in terms of information theory, of the type of classifier, resulting in a consistent and promising direction for future research.

IV. PEDESTRIAN DETECTION

Five classifiers, used for pedestrian detection, are discussed in this Section: Naive Bayes, GMMC, MCI-NN, FLDA and RBF-SVM.

A. Naive Bayes

Based on the assumption that each feature is statistically independent, the probability density function (*pdf*) that characterizes the object class m is modeled as the product of each feature-based *pdf*. A one-dimensional Gaussian $\theta_k(\mu_k, \sigma_k)$ was considered in modeling each *pdf*,

$$p(x_k|q_m, \theta_k) = \frac{1}{\sigma_k\sqrt{(2\pi)}}\exp[\frac{-(x_k-\mu_k)^2}{2\sigma_k^2}] \tag{4}$$

where μ_k is the mean and σ_k is the statistical variance for the k^{th} feature x_k, and q_m corresponds to the "object" class of interest, *i.e.* pedestrians q_1 and non-pedestrians q_2.

For the case q_1, the likelihood $\mathcal{L}$ is obtained by the normalization

$$\mathcal{L}(x_k|q_1) = \frac{p(x_k|q_1,\theta_k)}{p(x_k|q_1,\theta_k)+p(x_k|q_2,\theta_k)} \tag{5}$$

and therefore, the combined likelihood is expressed by

$$\mathcal{L}(x|q_1) = \prod_{k=1}^{d}\mathcal{L}(x_k|q_1) \tag{6}$$

where x corresponds to a d-dimensional feature vector.

B. GMMC

For the GMMC classifier, the likelihood is calculated considering a mixture of M Gaussian *pdf*, defined by $\Theta_i(\rho_i, \mu_i, \Sigma_i)$, where ρ_i is a weight-vector, such that $\sum_{i=1}^{M}\rho_i = 1$, μ_i is the d-dimensional mean vector, and Σ_i is the covariance matrix. The *pdf* for a single component i is modeled as

$$p(x|q_m, \Theta_i) = \frac{\exp[-\frac{1}{2}(x-\mu_i)^T(\Sigma_i)^{-1}(x-\mu_i)]}{\sqrt{(2\pi)^d}} \tag{7}$$

Finally, the likelihood is the linear composition

$$\mathcal{L}(x|q_1) = \sum_{i=1}^{M}\rho_i \cdot p(x|q_1, \Theta_i) \tag{8}$$

C. MCI-NN

Minimization of InterClass Interference (MCI) [14] is a maximum-margin based training algorithm for Neural Networks (NN). MCI aims to create a NN hidden layer output (*i.e.* feature space) where the patterns have a desirable statistical distribution. Regarding the neural architecture, the linear output layer is replaced by the Mahalanobis kernel in order to improve generalization. MCI is applicable on a neural network model with two sigmoidal hidden layers and one output non-linear layer:

$$yhf = \varphi(W_1 \cdot x + b_1) \tag{9}$$

$$yhs = \varphi(W_2 \cdot yhf + b_2) \tag{10}$$

$$\widehat{y} = \frac{d_2 - d_1}{d_2 + d_1} \tag{11}$$

where yhf is the output vector of the first hidden layer, yhs is the output vector of the second hidden layer, W_k $(k = 1, 2)$ is the synaptic weights matrix of the layer k, b_k is the bias vector of layer k, x is the input vector, $\varphi(.)$ is the sigmoid function, $d_m = (yhs - \mu_m)^T \Sigma^{-1} (yhs - \mu_m)$ is the Mahalanobis distance between yhs and μ_m, Σ is the covariance matrix over all the output vectors yhs, presented by the second hidden layer in response to the training data set, $\mu_m = \frac{1}{N_m} \sum_{i=1}^{N_m} yhs_m(i)$ is the prototype of Class m, N_m is the number of training patterns that belong to Class m, and $yhs_m(i)$ is the second hidden layer output for an input that belongs to Class m. Analyzing (11) we can observe that $\widehat{y}$ varies continuously from -1, for $yhs = \mu_2$, to 1, for $yhs = \mu_1$. This continuous approach enables ROC curves calculation. The MCI creates a hidden space where the Euclidean distance between the prototypes of each class is increased, and the patterns dispersion of each class is decreased. The goal is to maximize the objective function

$$J = (\mu_1 - \mu_2)^T (\mu_1 - \mu_2) - \delta_1^2 - \delta_2^2 \tag{12}$$

where, $\delta_m^2 = \sum_{i=1}^{N_m} (yh_m(i) - \mu_m)^T (yh_m(i) - \mu_m)$ is the deviation of Class m patterns in the hidden space. The weights and biases are updated based on the gradient ascendent algorithm.

D. FLDA

Let us consider w a vector of adjustable gains and $\{x_c\}$ the set of feature vectors that belong to Class c, $(c = 1, 2)$ with mean μ_c, and covariance $\sum_c$. The linear combination $w \cdot x_c$ has mean $w \cdot \mu_c$ and covariance $w^T \Sigma_c w$. The ratio, $J(w)$, of the variance *between* the classes, $\sigma_{\mathbf{b}}^2$, by the variance *within* the classes, $\sigma_{\mathbf{w}}^2$, is a suitable measure of separation between these two classes:

$$J(w) = \frac{\sigma_{\mathbf{b}}^2}{\sigma_{\mathbf{w}}^2} = \frac{(w \cdot (\mu_2 - \mu_1))^2}{w^T (\Sigma_1 + \Sigma_2) w} \tag{13}$$

To obtain the maximum separation between classes one has to find the vector w which solves the optimization problem

$$\max_w J(w) \tag{14}$$

whose solution is

$$w = (\Sigma_1 + \Sigma_2)^{-1} (\mu_2 - \mu_1) \tag{15}$$

To find the plane that best separates the data, the expression $w^T \mu_1 + b = -(w^T \mu_2 + b)$ has to be solved for the bias b.

E. SVM

Support Vector Machines (SVM) are based on the statistical theory of learning, developed by Vapnik [15]. This theory provides a set of principles to be followed in order to obtain classifiers with good generalization, defined as its ability to predict correctly the class of new data in the same area where the learning occurred. SVM is very sensitive to the margin parameter C [3], therefore, it is not appropriate to adjust this parameter based on the SVM performance on the test data set, since in this case information from the test data set will be carried to the SVM. The usual approach is to apply K-fold cross validation over the training data set.

V. RESULTS

The LIDAR-based pedestrian detection system was evaluated in terms of AUC, accuracy, and ROC curves. The data sets, summarized in Table II, were acquired in the ISR-UC *Campus* (http://www.isr.uc.pt/~cpremebida/PoloII-Google-map.pdf), under the following configuration:

1) Ibeo-based data set: the LIDAR was mounted approximately 52 cm above the ground, with Field of View (FOV) restricted to 180^o, horizontal angular resolution of 0.5^o, vertical resolution of $[-1.2^o, -0.4^o, 0.4^o, 1.2^o]$, and measurement range up to $35m$;
2) Sick-based data set: the LIDAR was mounted approximately 64,5 cm above the ground, 180^o of the FOV, horizontal angular resolution of 0.5^o, and part of the measurements ranging up to $8m$ and part up to $25m$.

The positives correspond to pedestrians in static or moving behavior, and the negatives consist of trees, vehicles, posts, walls, hydrants, poles, etc. The vehicle where the LIDARs were mounted, shown in Fig. 3, was driven with a maximum speed of 40Km/h approximately. The data sets and the corresponding ground truth, generated under user supervision, are available on the Web[4] for further comparisons and evaluations.

TABLE II
DATA SETS USED TO TRAIN AND TO EVALUATE THE CLASSIFIERS.

Ibeo-based data set				
Designation	Total	N pos.	N neg.	Description
$Data1_{ISR-UC}$	2614	1637	977	Training data set
$Data2_{ISR-UC}$	1000	500	500	Testing data set
Sick-based data set				
Designation	Total	N pos.	N neg.	Description
$Data3_{ISR-UC}$	2244	1184	1060	Training data set
$Data4_{ISR-UC}$	1000	500	500	Testing data set

A. Summary of the classifiers

The FLDA and the Naive-Bayes are base classifiers, not requiring parameters adjustments. Eventually, for the case of Naive-Bayes classifiers, the likelihood tends to zero depending on the feature distributions. Based on experiments during the training phase, the number of Gaussian components in the GMMC classifier was set to 4, and the margin parameter used in the RBF-SVM was 1000. Moreover, the MCI-NN was configured with 30 and 200 neurons in the first and second layers respectively.

[3]Margin parameter that determines the trade-off between maximization of the margin and minimization of the classification error [16]

[4]http://www.isr.uc.pt/~cpremebida/dataset_laser

Fig. 3. Electric vehicle and the sensors setup used in the data set acquisition.

B. Feature analysis

As a demonstration of the impact on the classification performance when the number of features (*nfea*) varies, consider the bar-graphs, Fig. 4 and Fig. 5, where the AUC and the accuracy (Acc) were used as classification performance metrics. The total number of features, restricted to 10, have been selected using the mRMR method. The best results for each classification method in terms of AUC, Acc and *nfea* are presented in Table III.

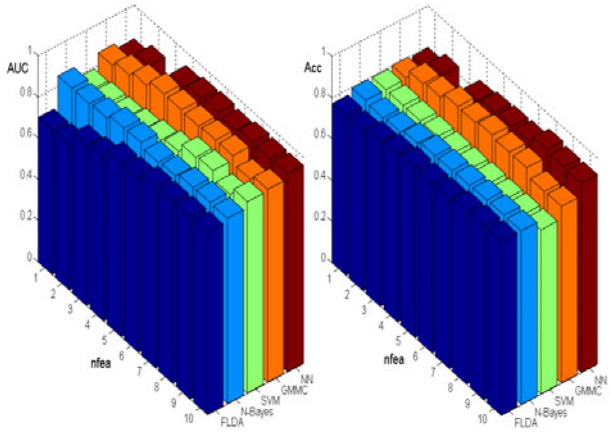

Fig. 4. Number of features vs classifier performance using the data set obtained with the Ibeo AlascaXT laser.

TABLE III

CLASSIFICATION PERFORMANCE: TESTING DATA SET

	Ibeo data set			Sick data set		
	AUC	Acc	$nfea$	AUC	Acc	$nfea$
FLDA	0.884	0.845	9	0.890	0.80	7
Naive-Bayes	0.903	0.843	9	0.932	0.855	1
RBF-SVM	0.928	0.796	8	0.965	0.904	9
GMMC	0.950	0.894	8	0.989	0.94	3
MCI-NN	0.963	0.931	8	0.968	0.943	9

C. Classification performance

To allow an appropriate analysis of the classification performance, ROC curves for the Ibeo and Sick data sets are displayed in Fig. 6 and Fig. 7 respectively. The FLDA, Naive-Bayes and RBF-SVM classifiers had, in both data sets, an analogous performance behavior, excepting the Naive-Bayes which, for the Sick data set, had achieved the best result with just one feature. On the other hand, the GMMC and the MCI-NN did not display much distinction on the performance nature for each data set; actually both classification methods achieved promising results.

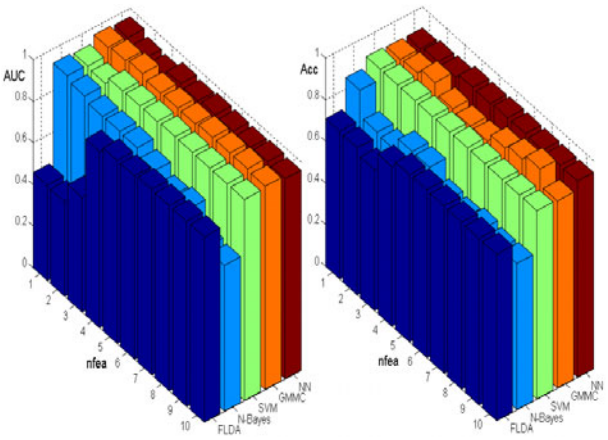

Fig. 5. Number of features vs classifier performance using the data set obtained with the Sick LMS200.

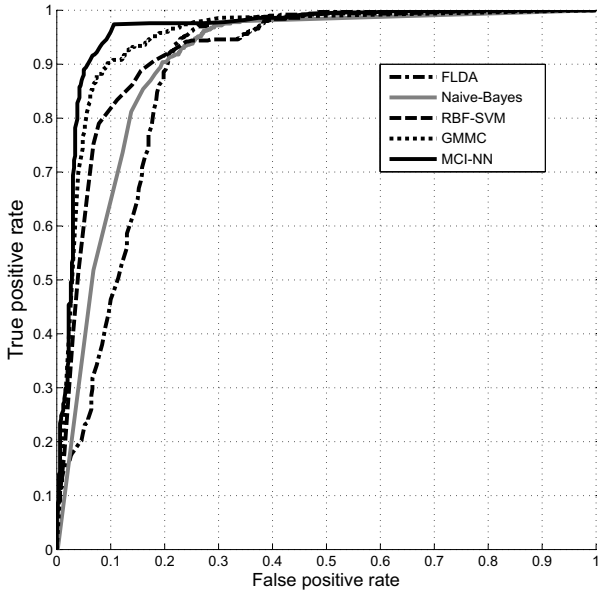

Fig. 6. ROC using Ibeo data set.

VI. CONCLUSIONS

A perception system is indispensable to assess the potential risk for the ego-vehicle and, more important than that, the risk for the vulnerable road users, specifically for the case of pedestrians. In this subject, many researches have addressed coherent solutions for pedestrian classification using, in most of the cases, a LIDAR as a prior object detector, hence the pedestrian classification decision was carried out by vision-based systems.

In this present work we have expanded on this subject and have presented as main contribution a relevant study on

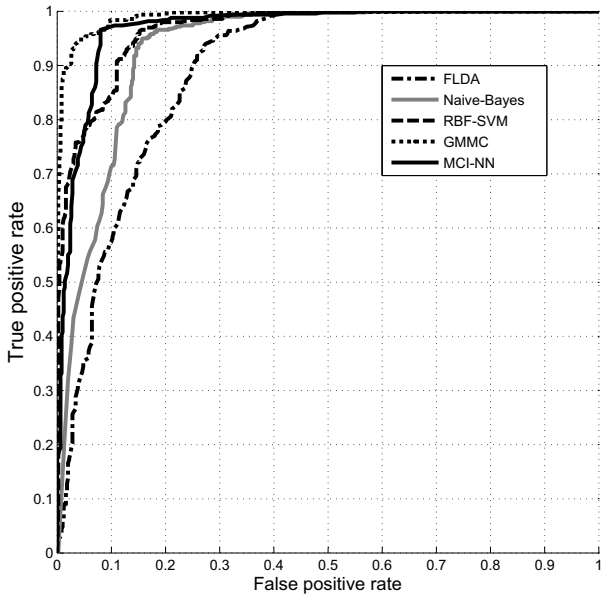

Fig. 7. ROC using Sick data set.

pedestrian detection in urban areas using only laser-based features, aiming to explore as much as possible LIDAR sensors, despite of merely using such sensors as prior object detector (object-hypothesis generator). Experiments with five classification techniques using data from an automotive and an industrial LIDAR were presented to demonstrate the effectiveness of such solution, and further comparisons can be made with the data sets that are online available for public usage.

An appropriate and feasible solution for object detection and classification in urban scenarios where many unpropitious and unpredictable circumstances can happen is still an open issue to be solved. In this context, here we have explored the potential of LIDAR in pedestrian classification, as a step forward to realistic applications where a perception system will face real circumstances of cluttered zones, oscillations, vibrations, weather influences, illumination changing, tracking and data association ambiguities, processing time constraints, normative requirements, etc.

VII. ACKNOWLEDGMENTS

This work is supported in part by Fundação para a Ciência e a Tecnologia de Portugal (FCT), under Grant PTDC/EEA-ACR/72226/2006. C.Premebida is supported by FCT under grant SFRH/BD/30288/2006 and O.Ludwig under grant SFRH/BD/44163/2008.

REFERENCES

[1] C. Premebida and U. Nunes. A multi-target tracking and gmm-classifier for intelligent vehicles. In *Intelligent Transportation Systems, ITSC. IEEE International Conference on*, pages 313–318, Sept. 2006.

[2] Tarak Gandhi and Mohan Manubhai Trivedi. Pedestrian protection systems: issues, survey, and challenges. *Intelligent Transportation Systems, IEEE Transactions on*, 8(3):413–430, 2007.

[3] K.O. Arras, O.M. Mozos, and W. Burgard. Using boosted features for the detection of people in 2d range data. In *Robotics and Automation, IROS. IEEE International Conference on*, pages 3402–3407, April 2007.

[4] J. Xavier, M. Pacheco, D. Castro, A. Ruano, and U. Nunes. Fast line, arc/circle and leg detection from laser scan data in a player driver. In *Robotics and Automation, ICRA. IEEE International Conference on*, pages 3930–3935, April 2005.

[5] K. Dietmayer, J. Sparbert, and D. Streller. Model based object classification and object tracking in traffic scenes from range images. In *Intelligent Vehicles Symposium, IVS. IEEE*, Tokyo, Japan 2001.

[6] D. Streller and K. Dietmayer. Object tracking and classification using a multiple hypothesis approach. In *Intelligent Vehicles Symposium, IVS. IEEE*, pages 808–812, June 2004.

[7] S. Gidel, P. Checchin, C. Blanc, T. Chateau, and L. Trassoudaine. Pedestrian detection method using a multilayer laserscanner: Application in urban environment. *Intelligent Robots and Systems, IROS. IEEE/RSJ International Conference on*, pages 173–178, Sept. 2008.

[8] L. Spinello and R. Siegwart. Human detection using multimodal and multidimensional features. In *Robotics and Automation, ICRA. IEEE International Conference on*, pages 3264–3269, May 2008.

[9] Cristiano Premebida, Oswaldo Ludwig, and Urbano Nunes. Lidar and vision-based pedestrian detection system. *Journal of Field Robotics*, 26(9), 2009.

[10] B. Douillard, D. Fox, and F. Ramos. A spatio-temporal probabilistic model for multi-sensor object recognition. In *Intelligent Robots and Systems, IROS. IEEE/RSJ International Conference on*, pages 2402–2408, 29 2007-Nov. 2 2007.

[11] C. Premebida and U. Nunes. Segmentation and geometric primitives extraction from 2d laser range data for mobile robot applications. In *Proc. 5th National Festival of Robotics, Scientific Meeting (ROBOTICA)*, Coimbra, Portugal, 2005.

[12] Jose E. Guivant, Favio R. Masson, and Eduardo M. Nebot. Simultaneous localization and map building using natural features and absolute information. *Robotics and Autonomous Systems*, 40(2-3):79 – 90, 2002.

[13] Hanchuan Peng, Fuhui Long, and C. Ding. Feature selection based on mutual information criteria of max-dependency, max-relevance, and min-redundancy. *Pattern Analysis and Machine Intelligence, IEEE Transactions on*, 27(8):1226–1238, Aug. 2005.

[14] O. Ludwig and U. Nunes. Improving the generalization properties of neural networks: an application to vehicle detection. In *Intelligent Transportation Systems, ITSC. IEEE International Conference on*, pages 310–315, Oct. 2008.

[15] Vladimir N. Vapnik. *Statistical Learning Theory*. John Wiley, 1998.

[16] Shigeo Abe. *Support Vector Machines for Pattern Classification (Advances in Pattern Recognition)*. Springer-Verlag New York, Inc., Secaucus, NJ, USA, 2005.